LETTERS

The human footprint in the carbon cycle of temperate and boreal forests

Federico Magnani[1], Maurizio Mencuccini[2], Marco Borghetti[3], Paul Berbigier[4], Frank Berninger[5], Sylvain Delzon[4], Achim Grelle[6], Pertti Hari[7], Paul G. Jarvis[2], Pasi Kolari[7], Andrew S. Kowalski[4], Harry Lankreijer[8], Beverly E. Law[9], Anders Lindroth[8], Denis Loustau[4], Giovanni Manca[10]†, John B. Moncrieff[2], Mark Rayment[2], Vanessa Tedeschi[3], Riccardo Valentini[10] & John Grace[2]

Temperate and boreal forests in the Northern Hemisphere cover an area of about 2×10^7 square kilometres and act as a substantial carbon sink (0.6–0.7 petagrams of carbon per year)[1]. Although forest expansion following agricultural abandonment is certainly responsible for an important fraction of this carbon sink activity, the additional effects on the carbon balance of established forests of increased atmospheric carbon dioxide, increasing temperatures, changes in management practices and nitrogen deposition are difficult to disentangle, despite an extensive network of measurement stations[2,3]. The relevance of this measurement effort has also been questioned[4], because spot measurements fail to take into account the role of disturbances, either natural (fire, pests, windstorms) or anthropogenic (forest harvesting). Here we show that the temporal dynamics following stand-replacing disturbances do indeed account for a very large fraction of the overall variability in forest carbon sequestration. After the confounding effects of disturbance have been factored out, however, forest net carbon sequestration is found to be overwhelmingly driven by nitrogen deposition, largely the result of anthropogenic activities[5]. The effect is always positive over the range of nitrogen deposition covered by currently available data sets, casting doubts on the risk of widespread ecosystem nitrogen saturation[6] under natural conditions. The results demonstrate that mankind is ultimately controlling the carbon balance of temperate and boreal forests, either directly (through forest management) or indirectly (through nitrogen deposition).

The life of forest ecosystems is punctuated by stand-replacing disturbances, mainly associated with fire or forest management. After each event, the forest is typically a net source of carbon (C) over the first years, followed by a broad peak in C sequestration (NEP, net ecosystem production; Fig. 1a) and gross primary production (GPP; Fig. 1b) in maturing forests. In older stands, NEP usually declines as a result of the age-related reduction in growth[7]. Age effects account for 92% of the total variability in NEP in five chronosequences analysed as part of the CARBOEUROPE project (http://www.bgc-jena.mpg.de/public/carboeur/), spanning from boreal coniferous to temperate broadleaf forests. Forested landscapes, however, are a patchwork of stands of different age, and the mean C sequestration at this scale is more closely approximated by the average NEP over the entire rotation, that is, between two subsequent stand-replacing events (NEP_{av}). When combining data from the five CARBOEUROPE chronosequences with several published literature data sets from boreal and temperate established forests (Table 1), NEP_{av} amounts to only 56% of peak NEP (38 ± 15% s.d. for individual forests; Fig. 2). Such a correction for disturbance effects could help reconcile flux- and inventory-based estimates of net C sequestration by terrestrial vegetation[4].

Because of their magnitude, age-related dynamics make it difficult to assess what other factors control forest C sequestration at the regional and global level[8]. We therefore filtered out the effects of age by taking the average of C fluxes over the entire rotation. Both ecosystem respiration (RE_{av}) and gross primary production (GPP_{av}) were positively correlated with mean annual temperature at the site ($R^2 = 0.83$ and 0.82, respectively); only one forest in the entire data set was known to be severely affected by water stress[9], which appeared to reduce in parallel both photosynthesis and respiration. The correlation with temperature improved significantly when this dry site was excluded from the analysis (Fig. 3a and b), so highlighting the primary role of heat and

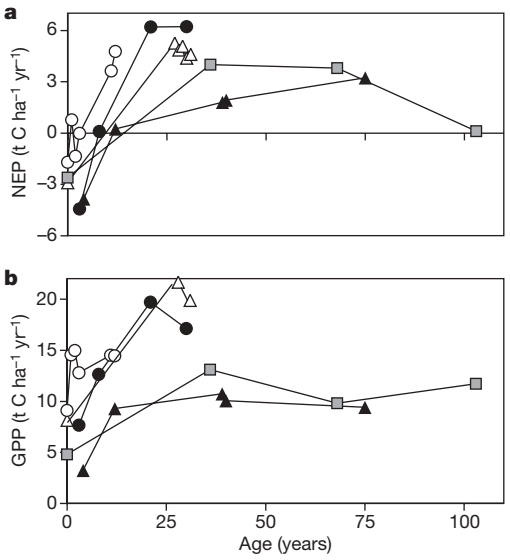

Figure 1 | Age-related dynamics of C balance components in forest ecosystems following disturbance. a, Dynamics of NEP; **b**, dynamics of GPP in five CARBOEUROPE chronosequences across Europe. Symbols refer to the following site codes (see Table 1): 7, black circles; 10, white triangles; 12, grey squares; 13, black triangles; 19, white circles.

[1]Department of Fruit Tree and Woody Plant Science, University of Bologna, Bologna I-40127, Italy. [2]School of GeoSciences, University of Edinburgh, Edinburgh EH93JU, UK. [3]Department of Crop Systems, Forestry and Environmental Sciences, University of Basilicata, Potenza I-85100, Italy. [4]INRA, UR1263 EPHYSE, Villenave d'Ornon F-33883, France. [5]Departement des Sciences Biologiques, University of Québec à Montréal, Montréal, Quebec, H3C 3P8, Canada. [6]Department of Ecology and Environmental Research, Swedish University of Agricultural Sciences, SE-75007 Uppsala, Sweden. [7]Department of Forest Ecology, University of Helsinki, FIN-00014 Helsinki, Finland. [8]Department of Physical Geography and Ecosystems Analysis, Lund University, S-223 62 Lund, Sweden. [9]College of Forestry, Oregon State University, Corvallis, OR 97331, USA. [10]Department of Forest Resources and Environment, University of Tuscia, Viterbo I-01100 Italy. †Present address: Institute for Environment and Sustainability—Climate Change Unit, Joint Research Center, European Commission, I-21020 Ispra, Italy.

Table 1 | Main site characteristics and C flux components of forest chronosequences used in the analysis

Main species	Site code	Age (years)	Latitude (° N)	Longitude (° E)	Data type	Disturbance type	GPP_{av} (t C ha^{-1} yr^{-1})	RE_{av} (t C ha^{-1} yr^{-1})	NEP_{av} (t C ha^{-1} yr^{-1})	Maximum NEP (t C ha^{-1} yr^{-1})	Reference
Fagus sylvatica	1	0–250*	51° 05′	10° 27′	EC	AB	15.6	10.7	4.9		23
	2	30–153	51° 20′	10° 22′	B	SW	16.1	11.5	4.6		24
Nothofagus solandrii	3	10–>160	43° 15′	171° 35′	B	WT			0.3		22
Picea mariana	4	3–151	55° 53′	−98° 20′	B	FF	6.6	6.2	0.4	1.1	25
	5	3–151	55° 53′	−98° 20′	B	FF	7.1	6.4	0.7	2.9	25
	6	11–130	55° 54′	−98° 28′	EC	FF	6.7	6.5	0.2	1.2	26
Picea sitchensis	7	3–30	55° 10′	2° 03′	EC, B	CC	15.4	12.7	2.7	5.5	†
Pinus banksiana	8	1–72	44° 35′	−84° 15′	B	FF			0.4	1.8	27
	9	0–79	53° 54′	−104° 39′	B	CC, FF	5.5	5.4	0.1	0.5	28
Pinus pinaster	10	0–50	44° 35′	0° 52′	EC, B	CC	18.3	14.8	3.6	6.5	†
Pinus ponderosa	11	9–316	44° 24′	−121° 36′	B	CC	7.8	7.2	0.6	1.6	9
Pinus sylvestris	12	0–103	60° 05′	17° 28′	EC, B	CC	10.1	8.5	1.6	3.7	†
	13	4–75	61° 51′	24° 17′	EC, B	CC	9.5	8.4	1.1	2.3	†
	14	12–266	60° 43′	89° 08′	B	FF	7.4	7.0	0.4	0.6	21
	15	14–215	60° 43′	89° 08′	B	FF	4.0	3.9	0.1	0.2	21
	16	2–383	60° 43′	89° 08′	B	FF	5.5	5.4	0.1	0.4	21
	17	2–95	60° 43′	89° 08′	B	FF	4.1	3.6	0.5	1.3	21
Pseudotsuga menziesii	18	0–500*	45° 49′	−121° 57′	B	AB	12.7	12.5	0.2		29
Quercus cerris	19	1–17	42° 24′	11° 55′	EC, B	CO	16.1	13.7	2.4	4.4	†
Tsuga martensiana	20	14–262	43° 30′	−122° 00′	B	PE			0.1	0.6	30

EC, eddy covariance; B, biomass; CC, clear-cut; CO, coppice; SW, shelterwood; AB, abandoned; FF, forest fire; PE, pests; WT, windthrow. *Uneven aged. †This study.

water stress in controlling the individual components of forest C balance. This confirms previous studies at the continental scale[2,3], although with much lower scatter owing to the removal of age effects. In contrast with GPP_{av} and RE_{av}, mean NEP ($NEP_{av} = GPP_{av} - RE_{av}$) is only weakly correlated with temperature (Fig. 3c). No correlation was found with either annual precipitation ($R^2 = 0.01$) or site latitude ($R^2 = 0.04$), leaving open the question of what could be driving C sequestration in boreal and temperate forests.

It was first recognized in the 1980s that human activities, by releasing into the atmosphere unprecedented amounts of active nitrogen (N), were not just altering the global N cycle[5], but also resulting in the eutrophication of large parts of the biosphere[10]. Boreal and temperate forest ecosystems are generally N-limited and the addition of N through wet and dry deposition has been hypothesized to result in the stimulation of forest growth and C sequestration[6]. Earlier model simulations suggested that N deposition could account for an increased C sequestration of 0.44–0.74 Pg yr^{-1}, mainly in temperate and boreal regions[11]. More recently, the relevance of N deposition for forest C sequestration has been questioned, on the basis of manipulation studies[12] and modelling extrapolation from N budgets[13]. In both studies, however, C sequestration was estimated from N fluxes themselves, assuming fixed C:N ratios. The relationship between N deposition and forest C sequestration has never been tested through direct observations across a range of forest conditions.

Using recently released gridded maps of N fluxes across Western Europe and North America[14], we found a tight relationship between average C sequestration and wet N deposition in the corresponding cell (Fig. 3d; $R^2 = 0.97$), which is largely obscured by age effects when data from individual stands are considered. We used wet rather than total N deposition because dry deposition was not measured directly, but derived from transfer models based on a limited data set of atmospheric concentrations, resulting in very large uncertainties[5]. The substantial net C sequestration by many temperate forests appears to be overwhelmingly determined by the additional input of N induced by human activities. We therefore hypothesize that the observed response of GPP_{av} and RE_{av} to temperature is mainly controlled by soil organic matter decomposition, which releases the nutrients needed for photosynthesis and growth, and that human activities, by adding an additional source of N readily available to plants, have determined an imbalance between the two components of the feed-back loop, so resulting in the net sequestration of C by forest ecosystems. Although a comprehensive analysis should consider in detail the distribution of existing forests and their uneven age structure, as well as the loss of C

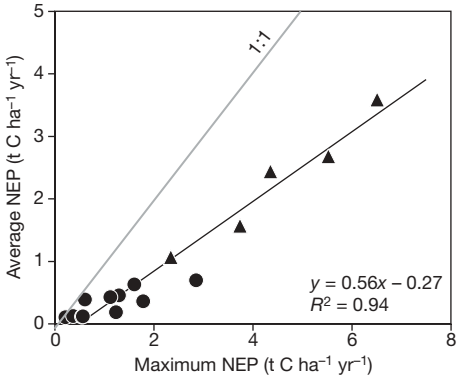

Figure 2 | Relationship between average NEP over the entire rotation and peak NEP in mature stands. Data from five CARBOEUROPE chronosequences (triangles) have been combined with eleven other literature data sets (see Table 1). Estimates of average and peak NEP are based on interpolated values of C fluxes; a linear function has been fitted by Type II regression ($n = 16$).

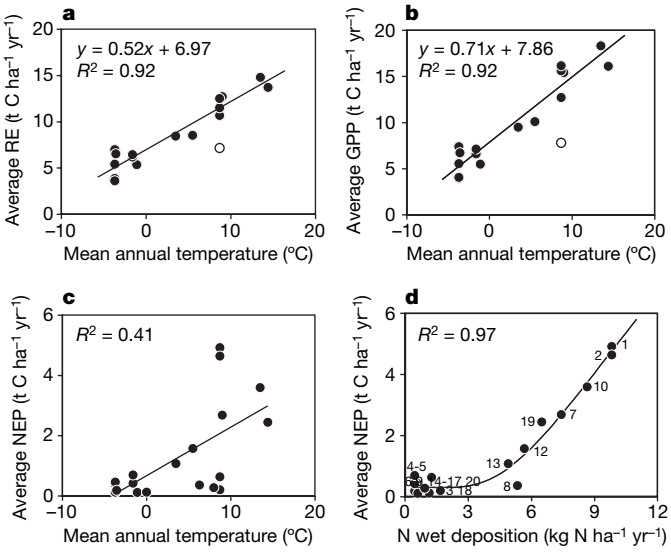

Figure 3 | Environmental control of average C exchange over an entire rotation. Linear relationships between average RE (**a**) and average ecosystem GPP (**b**) and mean annual temperature at the study sites. In both **a** and **b**, the only drought-prone site[9] (white circle) has been excluded from the analysis. **c**, Average NEP is only poorly correlated to temperature. **d**, Average NEP is strongly related to N deposition. Numbers refer to site codes in Table 1. An Arrhenius function has been empirically fitted onto the entire data set ($n = 20$).

through wildfire and logging, this could amount to an important fraction of the estimated C sink in the Northern Hemisphere[1].

The proposed mechanism of ecosystem response to N deposition implies that plants can readily access this additional nutrient source, in contrast with the results of several manipulative studies[12]. Under conditions of long-term, low-dose fertilization, however, plants are effective competitors for available N (ref. 15); moreover, their ability to compete for N would appear to increase with N availability, as the microbial demand for N becomes saturated by local organic sources with progressively lower C:N (ref. 15, 16). This could explain the increasing slope of the NEP_{av} response at high levels of N deposition (Fig. 3d), as more and more nutrients would be absorbed by plants and used for the production of woody biomass, with a high C:N ratio.

Are temperate and boreal forest ecosystems bound to become themselves saturated with N, resulting in forest dieback and a reduction in C sequestration[6]? Long-term studies of N enrichment in forests have demonstrated that ecosystem function responds to addition rate, rather than cumulated N input, and that although intermediate deposition levels could have beneficial effects, these could disappear at super-optimal N levels[17]. No signs of N saturation were apparent in our data set (Fig. 3d), which explored a broad range of wet deposition up to 9.8 kg N ha^{-1} yr^{-1} (~15 kg N ha^{-1} yr^{-1} of total N deposition), representative of more than 90% of the overall surface of Western Europe and the conterminous United States[14]. Long-term manipulation studies indicate that only at N addition levels of 50–60 kg N ha^{-1} yr^{-1} do clear signs of soil acidification, nutrient imbalances and tree damage become apparent[17,18]. Although these values are in excess of current maximum levels of atmospheric N deposition[14], even higher rates are occasionally recorded and could occur in the future over entire regions[5]. Further chronosequence studies in selected areas with high N deposition could help us understand if the beneficial effects of N fertilization on the terrestrial C sink can be expected to persist over the next century.

METHODS SUMMARY

Both C stocks and C fluxes[2] were measured in five representative forest chronosequences throughout Europe (Table 1), which comprised newly harvested, young and mature stands in the same locality. At each site, GPP and RE were also computed from NEP data. Data from 13 additional chronosequences and two uneven-aged stands were drawn from the literature (Table 1). When estimates based on the eddy-covariance technique were not available, GPP was derived from annual net primary production (NPP), assuming a constant relationship[19], and RE estimated as the difference from NEP. All chronosequences were located either in natural forests or in plantations at least at second rotation and were not actively fertilized.

The chronosequence approach quantifies ecosystem C sink capacity at several stages in forest development; modelling tools were used to interpolate the resulting information over the entire rotation. A process-based approach was applied in the case of CARBOEUROPE chronosequences, for which direct flux and stock data were available, by linking two well-documented and tested ecosystem models[19,20]. In the case of literature chronosequences, flux integrals over the entire rotation were obtained by fitting suitable empirical equations[9,21] onto flux or ecosystem C data. In just one case[22], because of the limited sample size, NEP_{av} was estimated from the difference in ecosystem C between the newly regenerated stand and the old stand.

Estimates of N wet deposition in 1990 for sites in Western Europe and the conterminous United States were derived from recently published gridded maps[14]. Additional data for 1993 for the rest of the globe were derived from model simulations[5]; estimates of wet N deposition were then derived from modelled values of total N deposition, based on a correlation of values in the previous data set.

Full Methods and any associated references are available in the online version of the paper at www.nature.com/nature.

Received 13 November 2006; accepted 11 April 2007.

1. Goodale, C. L. *et al.* Forest carbon sinks in the Northern Hemisphere. *Ecol. Appl.* **12,** 891–899 (2002).
2. Valentini, R. *et al.* Respiration as the main determinant of carbon balance in European forests. *Nature* **404,** 861–865 (2000).
3. Law, B. E. *et al.* Environmental controls over carbon dioxide and water vapor exchange of terrestrial vegetation. *Agric. For. Meteorol.* **113,** 97–120 (2002).
4. Körner, C. Slow in, rapid out: carbon flux studies and Kyoto targets. *Science* **300,** 1242–1243 (2003).
5. Galloway, J. N. *et al.* Nitrogen cycles: past, present, and future. *Biogeochemistry* **70,** 153–226 (2004).
6. Aber, J. D. *et al.* Nitrogen saturation in temperate forest ecosystems. *Bioscience* **48,** 921–934 (1998).
7. Pregitzer, K. S. & Euskirchen, E. S. Carbon cycling and storage in world forests: biome patterns related to forest age. *Glob. Change Biol.* **10,** 2052–2077 (2004).
8. Thornton, P. E. *et al.* Modeling and measuring the effects of disturbance history and climate on carbon and water budgets in evergreen needleleaf forests. *Agric. For. Meteorol.* **113,** 185–222 (2002).
9. Law, B. E., Sun, O. J., Campbell, J., vanTuyl, S. & Thornton, P. E. Changes in carbon storage and fluxes in a chronosequence of ponderosa pine. *Glob. Change Biol.* **9,** 510–524 (2003).
10. Peterson, B. J. & Melillo, J. M. The potential storage of carbon caused by eutrophication of the biosphere. *Tellus B* **37,** 117–127 (1985).
11. Townsend, A. R., Braswell, B. H., Holland, E. A. & Penner, J. E. Spatial and temporal patterns in terrestrial carbon storage due to deposition of fossil fuel nitrogen. *Ecol. Appl.* **6,** 806–814 (1996).
12. Nadelhoffer, K. J. *et al.* Nitrogen deposition makes a minor contribution to carbon sequestration in temperate forests. *Nature* **398,** 145–148 (1999).
13. De Vries, W., Reinds, G. J., Gundersen, P. & Sterba, H. The impact of nitrogen deposition on carbon sequestration in European forests and forest soils. *Glob. Change Biol.* **12,** 1151–1173 (2006).
14. Holland, E. A., Braswell, B. H., Sulzman, J. & Lamarque, J. F. Nitrogen deposition onto the United States and Western Europe: synthesis of observations and models. *Ecol. Appl.* **15,** 38–57 (2005).
15. Johnson, D. W. Nitrogen-retention in forest soils. *J. Environ. Qual.* **21,** 1–12 (1992).
16. Schimel, J. P. & Bennett, J. Nitrogen mineralization: Challenges of a changing paradigm. *Ecology* **85,** 591–602 (2004).
17. Högberg, P., Fan, H., Quist, M., Binkley, D. & Tamm, C. O. Tree growth and soil acidification in response to 30 years of experimental nitrogen loading on boreal forest. *Glob. Change Biol.* **12,** 489–499 (2006).
18. Magill, A. H. *et al.* Ecosystem response to 15 years of chronic nitrogen additions at the Harvard Forest LTER, Massachusetts, USA. *For. Ecol. Manage.* **196,** 7–28 (2004).
19. Landsberg, J. J. & Waring, R. H. A generalized model of forest productivity using simplified concepts of radiation-use efficiency, carbon balance and partitioning. *For. Ecol. Manage.* **95,** 209–228 (1997).
20. Andrén, O. & Kätterer, T. ICBM: the introductory carbon balance model for exploration of soil carbon balances. *Ecol. Appl.* **7,** 1226–1236 (1997).
21. Wirth, C., Czimczik, C. I. & Schulze, E.-D. Beyond annual budgets: carbon flux at different temporal scales in fire-prone Siberian Scots pine forests. *Tellus B* **54,** 611–630 (2002).
22. Davis, M. R., Allen, R. B. & Clinton, P. W. Carbon storage along a stand development sequence in a New Zealand *Nothofagus* forest. *For. Ecol. Manage.* **177,** 313–321 (2003).
23. Knohl, A., Schulze, E.-D., Kolle, O. & Buchmann, N. Large carbon uptake by an unmanaged 250-year-old deciduous forest in Central Germany. *Agric. For. Meteorol.* **118,** 151–167 (2003).
24. Mund, M. *Carbon Pools of European Beech Forests (*Fagus sylvatica*) Under Different Silvicultural Management.* PhD thesis, Georg-August-Universität Göttingen (2004).
25. Bond-Lamberty, B., Wang, C. & Gower, S. T. Net primary production and net ecosystem production of a boreal black spruce wildfire chronosequence. *Glob. Change Biol.* **10,** 473–487 (2004).
26. Litvak, M., Miller, S., Wofsy, S. C. & Goulden, M. Effect of stand age on whole ecosystem CO_2 exchange in the Canadian boreal forest. *J. Geophys. Res.* **108** (D3), 8225 (2003).
27. Rothstein, D. E., Yermakov, Z. & Buell, A. L. Loss and recovery of ecosystem carbon pools following stand-replacing wildfire in Michigan jack pine forests. *Can. J. For. Res.* **34,** 1908–1918 (2004).
28. Howard, E. A., Gower, S. T., Foley, J. A. & Kucharik, C. J. Effects of logging on carbon dynamics of a jack pine forest in Saskatchewan, Canada. *Glob. Change Biol.* **10,** 1267–1284 (2004).
29. Harmon, M. E. *et al.* Production, respiration, and overall carbon balance in an old-growth Pseudotsuga-Tsuga forest ecosystem. *Ecosystems* **7,** 498–512 (2004).
30. Boone, R. D., Sollins, P. & Cromack, K. Stand and soil changes along a mountain hemlock death and regrowth sequence. *Ecology* **69,** 714–722 (1988).

Supplementary Information is linked to the online version of the paper at www.nature.com/nature.

Acknowledgements This work was supported by the European Commission (General Directorate XII, CARBO-AGE project in the CARBOEUROPE cluster) and further supported by several national programmes. F.M. was also supported by the MIUR CarboItaly Project and by Società Produttori Sementi (Fondazione Cassa di Risparmio in Bologna) through the 'Selvicoltura' project.

Author Information Reprints and permissions information is available at www.nature.com/reprints. The authors declare no competing financial interests. Correspondence and requests for materials should be addressed to F.M. (federico.magnani@unibo.it).

METHODS

The analysis was based on a combination of measurements from five European chronosequences, collected as part of the CARBOEUROPE project, and literature data from a total of 15 chronosequences or uneven aged stands. A chronosequence is defined as a collection of forest stands of different age but otherwise homogeneous for plant material and environmental conditions; the footprint area of a chronosequence is larger than those generally studied in manipulation experiments, partly compensating for the lack of experimental replicates. All chronosequences were located either in natural forests or in plantations at least at second rotation and were not actively fertilized.

Description of CARBOEUROPE chronosequences. We identified five representative managed forests throughout Europe (see Table 1), which comprised newly harvested, young and mature stands in the same locality. The UK series consists of stands of *Picea sitchensis* at Harwood in northwest England; soils are predominantly peaty gleys, formed over glacial tills. The forest is managed by clear-cutting; the usual rotation is 40 years, and the data reported here are from the second rotation. Measurements were taken in stands 0, 7, 21 and 30 years old. The Italian site is a coppice with standards of *Quercus cerris* at Roccarespampani in Central Italy. The soil is a Luvisol on a volcanic bedrock. The rotation length is 15–20 years. The ages of the available stands span the entire rotation: data are available for ages 1, 4, 10 and 17 years. The Finnish series consists of stands of *Pinus sylvestris* at Juupajoki in Southern Finland, on sandy glacial till of moderate fertility; the 40-year-old stand is 5 km away, in Hyytiälä, on coarse sandy glacial till. The rotation length is typically 80 years; the stands analysed are 3, 10, 40 and 75 years old. The Swedish sites are in Central Sweden, at Skyttorp (0, 30 and 60 years) and at Norunda (100 years); all the stands are dominated by *P. sylvestris*. The typical rotation length is about 100 years. The soil is a deep, boulder-rich sandy glacial till. The French site is part of Les Landes forest in southwestern France, and consists of mono-specific *Pinus pinaster* stands 0, 16, 26 and 50 years old on spodic sands. The typical rotation length is 50 years at the site.

Both C stocks (in soils, litter, woody debris and vegetation) and C fluxes were measured at each stand in the chronosequence; each stand in a chronosequence was large enough to satisfy conditions for measurement of CO_2 fluxes by the eddy covariance technique[31]. At each site, GPP and RE were also computed from NEP data, by assuming that respiration by day is the same as that at night after adjustment for the effect of the diurnal temperature cycle.

Literature data sets. Data from 13 additional chronosequences and 2 uneven-aged stands from boreal and temperate forests were drawn from the literature (see Table 1). The data set comprised only one chronosequence from the Southern Hemisphere. Direct measurements of NEP or ecosystem C were used for the estimation of average NEP over the entire rotation. C flux estimates in literature chronosequences were based either on the eddy-covariance technique or on biometric measurements (as detailed in Supplementary Table 1, see Supplementary Information). When data were provided only in graphical format, the relevant figure was captured from the electronic paper using commercial software (Paint Shop Pro 4.12, JASC) and individual datapoints digitized using the Un-Scan-It 5.0 dedicated software (Silk Scientific). When estimates based on the eddy-covariance technique were not available, GPP was derived from estimates of annual NPP, assuming a constant ratio[32], and RE was estimated as the difference from NEP.

Computation of average C fluxes in CARBOEUROPE chronosequences. Although the chronosequence approach quantifies ecosystem C sink capacity at several stages in forest development, modelling tools are needed to interpolate the resulting information over the entire rotation. While such an integration procedure is needed to correct for any biases resulting from the limited sample size of each chronosequence, very similar results are obtained when raw means (and maxima) of field measurements are used instead (see Supplementary Information). A process-based approach was applied in the case of CARBOEUROPE chronosequences, for which direct flux and stock data were available, by linking two well-documented and tested ecosystem models. The 3PG-3 model stems from the combination of the 3PG (use of Physiological Principles in Predicting Growth) model[19], to represent the NPP and growth of a forest stand, and the ICBM (Introductory Carbon Balance Model) model[20] for belowground C dynamics. The two models have been extensively documented and tested[19,20,33–37]. In addition, a third component has been added to represent the C exchange by the forest understorey (hence the suffix in 3PG-3), with a structure derived from the 3PG model with further simplifications.

General model structure. Because the aim of the model is to capture age-related differences among stands in a chronosequence, all experiencing the same conditions, the model overlooks the detailed response of primary production to individual environment factors, capturing it as a single reduction coefficient for the whole chronosequence irrespective of stand age. A single reduction factor also captures the response of soil heterotrophic respiration to the soil environment (temperature, humidity, soil texture), irrespective of stand age. Age is assumed to have a direct effect (that is independent from the dynamics of C stocks) only on light-use efficiency, as described below. Because the seasonal dynamics of environmental factors are neglected, an annual time step is adopted throughout.

NEP. The representation of forest NPP is based on the light-use efficiency approach[38]. The amount of photosynthetically active radiation absorbed by the stand over the year Φ_{pa} is a function of incoming radiation Φ_p and stand foliage C (C_f), following Beer's law:

$$\Phi_{pa} = \Phi_p(1-a)[1-\exp(-k \times SLA \times C_f)] \quad (1)$$

where a is canopy albedo, k is a light extinction coefficient (of value 0.5 for spherically distributed leaves) and SLA is foliage-specific leaf area (expressed in terms of leaf C content). Stand GPP is assumed to be linearly proportional to absorbed light:

$$GPP = \varepsilon \Phi_{pa} \quad (2)$$

Radiation light-use efficiency ε is reduced below its potential value ε_0 as a result of environmental and age-related effects:

$$\varepsilon = \varepsilon_0 f_{age} f_{tot} \quad (3)$$

The empirical parameter f_{tot} captures the combined effects of all environmental factors over the entire season and is assumed to be independent of stand age. The direct effects of age A are captured by the parameter f_{age}, defined as[19]:

$$f_{age} = \frac{1}{1+(A/A_{0.5})^4} \quad (4)$$

where the parameter $A_{0.5}$ is the age corresponding to a 50% reduction in light-use efficiency. Stand NPP is finally assumed to be a constant fraction of GPP[32]. The same approach is applied to understorey primary production. The amount of light reaching the understorey Φ_p^{und}, however, is first reduced by overstorey interception. Moreover, the light-use efficiency of the understorey is not reduced by age but only by the environment through the reduction factor f_{tot}^{und}.

Growth and litter production. Available C is assumed to be allocated between foliage (C_f), fine root (C_r) and woody biomass (C_w; including coarse roots and stumps) in proportion to allocation coefficients η_f, η_r and η_w, respectively. A constant value is assumed for allocation to foliage[39]. Allocation to roots, on the contrary, is assumed to increase in response to both environmental stress and age, in parallel with the reduction in light-use efficiency:

$$\eta_r = \frac{0.8}{1+2.5m \times f_{tot} f_{age}} \quad (5)$$

The empirical parameter m captures the effects of soil fertility on fine root growth, and increases with soil fertility. Allocation to wood production is represented as residual growth. Annual changes in the i-th tree compartment (foliage, fine root and woody tissues) are represented as the difference between new growth and litter losses:

$$\frac{\Delta C_i}{\Delta t} = NPP\eta_i - C_i\gamma_i \quad (6)$$

where the parameter γ_i represents the annual mortality of the i-th compartment and is equal to zero in the case of woody biomass. Steady-state conditions are assumed for the understorey; understorey litter production is therefore assumed to be equal to the corresponding NPP_{und}.

Soil respiration and net ecosystem exchange. The representation of soil organic matter (SOM) dynamics is based on the two-compartment ICBM model[20]. A young (that is, readily decomposable) and an old (that is, refractory) SOM compartment, with widely different residence times, are distinguished in the model.

The annual change in the biomass Y of the young SOM compartment is the difference of litter input (from trees and the understorey) and young SOM decomposition, which is assumed to be proportional to Y:

$$\frac{\Delta Y}{\Delta t} = (C_f\gamma_f + C_r\gamma_r + NPP_{und}) - rk_1 Y \quad (7)$$

The empirical parameter r captures the combined effects of temperature, humidity and soil texture on the decomposition parameter k_1, which represents unit Y decomposition under standard conditions. Young SOM decomposition is partly lost as respiration, the remaining being transferred to the old SOM compartment

through humification. Young SOM respiration is expressed as:

$$R^{y}_{SOM} = (1-h)rk_1 Y \quad (8)$$

where h is a humification coefficient. The annual change in old SOM biomass O is therefore equal to:

$$\frac{\Delta O}{\Delta t} = r(k_1 Yh - k_2 O) \quad (9)$$

where k_2 represents unit O decomposition under standard conditions, modulated by the same parameter r as a result of the environment. Old SOM respiration can be expressed as:

$$R^{o}_{SOM} = rk_2 O \quad (10)$$

NEP is the difference between tree and understorey NPP and the heterotrophic respiration from young and old SOM:

$$NEP = NPP + NPP_{und} - R^{y}_{SOM} - R^{o}_{SOM} \quad (11)$$

Model fitting procedure. The combined model was implemented in Fortran 95, calibrated independently for each chronosequence on measurements available for a limited number of ages and used to estimate C fluxes at every age in the chronosequence. The procedure made it possible to compute average fluxes over the entire rotation without the risks coming from the limited sample size. In contrast with more empirical equations, such a process-based model can represent coherently and at the same time all of the main C-cycle variables that are amenable to direct measurement. The model was therefore calibrated so as best to represent the values of annual fluxes (NEP and GPP) and C stocks (C_f, C_r, C_w, total SOM) measured in individual stands of the chronosequence. The ability of the model to represent all these variables at the same time increased the confidence in model estimates.

To include these non-commensurate sources of information in the calibration process, the multi-objective global optimization approach described in ref. 40 was adopted. Before model calibration, each variable was normalized by its mean and variance, so as to achieve the conditions of zero mean and constant variance among variables, which is a pre-condition for the application of the overall Maximum Likelihood Estimator as an objective function.

A total of seven model parameters (f_{tot}, f^{und}_{tot}, $A_{0.5}$, γ_r, m, h, r), plus three initial values of state variables (C_f, Y, O), were estimated for each chronosequence, leaving a number of degrees of freedom ranging between 9 and 21, depending on the chronosequence considered. All other parameters and input variables were derived from direct field measurements. Overall, the model explained 91% of the variability in C stocks and fluxes within each chronosequence.

Computation of average C fluxes in literature chronosequences. If not already available, flux integrals over the entire rotation were obtained by fitting onto flux data the empirical equation proposed by ref. 9:

$$NEP = -a_1 + a_2 \exp\left\{-0.5[\ln(A/a_3)/a_4]^2\right\} \quad (12)$$

Alternatively, the empirical equation proposed by ref. 21 was fitted onto total ecosystem C data:

$$C_{eco} = b_1 + [b_2 \exp(-b_3 A)] + [b_4 A/(A+b_5)] \quad (13)$$

and annual NEP computed as the difference in ecosystem C between subsequent years. The two empirical models were fitted on experimental data with the NLIN procedure in the SAS 9.00 statistical package (SAS Institute). Average NEP over the rotation was computed as the mean of annual values between age zero and the maximum age in the chronosequence. In just one case[22], because of the limited sample size, average NEP was estimated from the difference in ecosystem C between the newly regenerated and the old stand. Although its omission does not have any appreciable effects on the results, this *Nothofagus* chronosequence has been included in the analysis because it is one of the few broadleaved forests and the only one from the Southern Hemisphere.

Annual GPP values were also integrated over the entire rotation, using the same function presented in equation (12). RE_{av} was computed as the difference between GPP_{av} and NEP_{av}. A detailed description of data type and integration procedures is presented in Supplementary Table 1 (see Supplementary Information).

Computation of N wet deposition. Estimates of N wet deposition in 1990 for sites in western Europe and the conterminous USA were derived from recently published gridded maps with $0.5^\circ \times 0.5^\circ$ resolution derived from interpolated (krieged) ground data[14] (available at http://www.daac.ornl.gov), referring to the nearest node in the map (see Supplementary Fig. 1). Total wet deposition was computed as the sum of aqueous NO_3^- and NH_4^+ fields, which were available for both regions. An estimate of total (modelled) N deposition was obtained as the sum of wet deposition and of the fields for deposition of NO_2, NH_4, HNO_3 and NO_3^-. In the case of Europe, because only the sum of nitric acid and particulate nitrate was measured, the relative fields represent end-members assuming only one species[14] and we took the average value. In the case of the US data set, NO_2 deposition rates were not available and their contribution to total N deposition was estimated from a regression of European values.

Additional data for 1993 for the rest of the globe were derived from model simulations[5,41]; estimates of wet N deposition were then derived from modelled values of total N deposition, based on a correlation of values from Western Europe in the previous data set (see Supplementary Fig. 2). The same correction factor was used in the comparison with N fertilization rates in manipulation experiments.

Statistical analyses. All statistical analyses were carried out using the SAS 9.00 statistical package (SAS Institute).

31. Aubinet, M. *et al.* Estimates of the annual net carbon and water exchange of forests: the Euroflux methodology. *Adv. Ecol. Res* **30,** 113–175 (2000).
32. Waring, R. H., Landsberg, J. J. & Williams, M. Net primary production of forests: a constant fraction of gross primary production? *Tree Physiol.* **18,** 129–134 (1998).
33. Coops, N. C., Waring, R. H. & Landsberg, J. J. Assessing forest productivity in Australia and New Zealand using a physiologically-based model driven with averaged monthly weather data and satellite-derived estimates of canopy photosynthetic capacity. *For. Ecol. Manage.* **104,** 113–127 (1998).
34. Paul, K. I., Polglase, P. J. & Richards, G. P. Predicted change in soil carbon following afforestation or reforestation, and analysis of controlling factors by linking a C accounting model (CAMFor) to models of forest growth (3PG), litter decomposition (GENDEC) and soil C turnover (RothC). *For. Ecol. Manage.* **177,** 485–501 (2003).
35. Law, B. E., Waring, R. H., Anthoni, P. M. & Abers, J. D. Measurements of gross and net ecosystem productivity and water vapour exchange of a *Pinus ponderosa* ecosystem, and an evaluation of two generalized models. *Glob. Change Biol.* **6,** 155–168 (2000).
36. Landsberg, J. J., Waring, R. H. & Coops, N. C. Performance of the forest productivity model 3-PG applied to a wide range of forest types. *For. Ecol. Manage.* **172,** 199–214 (2003).
37. Kätterer, T. & Andrén, O. The ICBM family of analytically solved models of soil carbon, nitrogen and microbial biomass dynamics. Descriptions and applications examples. *Ecol. Model.* **136,** 191–207 (2001).
38. Landsberg, J. J. *et al.* in *The Use of Remote Sensing in the Modeling of Forest Productivity* (eds Gholz, H. L., Nakane, K. & Shimoda, H.) 273–298 (Kluwer Academic, Dordrecht, 1996).
39. Santantonio, D. in *Biomass Production by Fast-Growing Trees* (eds Pereira, J. S. & Landsberg, J. J.) 57–72 (Kluwer Academic, Dordrecht, 1989).
40. Yapo, P. O., Gupta, H. V. & Sorooshian, S. Multi-objective global optimization for hydrologic models. *J. Hydrol.* **204,** 83–97 (1998).
41. Dentener, F. J. *Global Maps of Atmospheric Nitrogen Deposition, 1860, 1993, and 2050. Data set.* ⟨http://daac.ornl.gov/⟩. (Oak Ridge National Laboratory Distributed Active Archive Center, Oak Ridge, Tennessee, 2006).